Analog and Digital Functionalities of Composite-Resonator Vertical-Cavity Lasers

Chen Chen, *Student Member, IEEE*, and Kent D. Choquette, *Fellow, IEEE*

***Abstract*—Different modulation approaches for the composite-resonator vertical-cavity laser are described, with an emphasis on direct modulation using either one or both cavities. It is also observed that the unique properties of this device form the basis for analog and digital functionalities. Experimental demonstrations are also shown of multilevel amplitude modulation, preemphasis for direct modulation, microwave signal mixing, and synchronous electrical and optical signaling, none of which can be achieved using a conventional vertical-cavity surface-emitting laser.**

***Index Terms*—Coupled cavity, high-speed modulation, semiconductor lasers, vertical-cavity surface-emitting lasers (VCSELs).**

I. Introduction

THE vertical-cavity surface-emitting laser (VCSEL) has been widely used in short to midhaul data communication networks, due to its low-cost manufacture, low-power operation, high-speed modulation, and its ability for 2-D array integration [1]. During the last decade, a primary focus of VCSEL research was to achieve higher modulation bandwidth. Meanwhile, the VCSEL with two optically coupled cavities, which is known as the composite-resonator vertical-cavity laser (CRVCL), has also exhibited potential to enable new modulation concepts and thus to achieve high-speed modulation [2]–[5]. For emerging applications such as data centers, access networks, and radio-over-fiber transmission, additional optical functionality and lower power consumption will be demanded. Due to the unique properties of a coupled-cavity structure, the CRVCL may satisfy these demands by offering additional functionality and flexibility over a conventional VCSEL.

Unlike a conventional VCSEL, for which laser output can be varied only by direct modulation in a single-laser cavity, the CRVCL has the flexibility to modulate laser output using several different approaches. In this paper, we provide an overview of the modulation approaches for the CRVCL. For each modulation approach, the unique modulation characteristics are found from rate equation analysis and compared to modulation experiments. We also demonstrate several novel analog and digital applications for the CRVCL.

The paper is organized as follows: in Section II, we describe the modulation properties of the CRVCL with an emphasis on the direct modulation approaches. The CRVCL can modulate its light output through either or both of its cavities. The asymmetries between the coupled cavities are found to play a significant role in determining the CRVCL modulation response. With direct modulation in only one cavity, we demonstrate a maximum small-signal modulation bandwidth of 23 GHz. With direct modulation in both cavities, the CRVCL enables the engineering of the modulation response by varying the amplitude and phase difference between the modulation currents. The special condition of push--pull modulation represents as a new paradigm of laser modulation, aiming to achieve a very wide modulation bandwidth with low power consumption. In Section III, several new analog and digital functionalities of a CRVCL are presented with experimental demonstrations to address different issues in optical communications and other optical transmission applications.

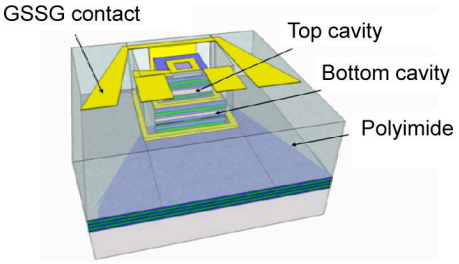

Fig. 1. Schematic of a CRVCL with a GSSG coplanar contact on the planarized surface.

II. Modulation Approaches

Unlike a conventional VCSEL, the photon population within a CRVCL is coupled to the carrier populations in both cavities simultaneously. The laser output of the CRVCL can be varied by applying electrical modulation to either or both of the coupled cavities. Fig. 1 illustrates the CRVCL structure used in our study. The CRVCL consists of a monolithic bottom p-type distributed Bragg reflector (DBR), a middle n-type DBR, and an upper p-type DBR. The two laser cavities, which are separated by the middle DBR mirror, are optically coupled but electrically independent. A ground-signal-signal-ground (GSSG) coplanar contact is used, in order to facilitate high-speed signaling into both optical cavities. The details about the CRVCL fabrication procedure can be found in [6].

For high-speed characterization, small-signal modulation characteristics of the CRVCL are measured using a network

Manuscript received September 16, 2009; revised December 07, 2009. First published February 08, 2010; current version published March 05, 2010. This work was supported in part by the Defense Advanced Research Projects Agency under Contract W31P4Q-07-C-0284.

C. Chen was with the Department of Electrical and Computer Engineering, University of Illinois, Urbana, IL 61801 USA. He is now with the Photonics Systems Group, Department of Electrical and Computer Engineering, McGill University, Montreal, QC H3A-2A7, Canada (e-mail: chen.chen4@mail.mcgill.ca).

K. D. Choquette is with the Department of Electrical and Computer Engineering, University of Illinois, Urbana, IL 61801 USA (e-mail: choquett@illinois.edu).

Color versions of one or more of the figures in this paper are available online at http://ieeexplore.ieee.org.

Digital Object Identifier 10.1109/JLT.2010.2041747

analyzer; large-signal modulation characteristics are obtained using a pattern generator and an oscilloscope. The maximum data rate from the pattern generator is 2.5 Gb/s. A cleaved 62.5/125 μm graded-index multimode fiber and a high-speed photodetector are used to collect output light from the CRVCL under test. A variable RF attenuator is used to adjust the amplitude difference between the modulation signals, when both cavities are under simultaneous modulation.

A. Single-Cavity Direct Modulation

The simplest approach to induce light modulation from a CRVCL is to apply direct modulation to one of the coupled cavities. The rate equations for the CRVCL were solved in prior work to study the laser dynamics under direct modulation [2], [7]. It was found that the direct modulation response through the top cavity can be expressed in (1) and (2), at the bottom of this page. In (1) and (2), the subscript $k = 1$, and 2 refer to the top and bottom cavity, respectively. Γ_k is the optical confinement factor, v_k is the group velocity of the optical mode in the material (cm/s), g'_k is the differential gain (cm^{-2}), S_0 is the photon density (1/cm^3) in a single longitudinal and transverse mode, d_k is the gain region thickness (cm), τ_k is the carrier lifetime (s), g_k is the material gain (cm^{-1}), ξ_k is the percentage of the optical standing wave overlapping with the respective cavity, q is the elementary charge (C), ω is the angular modulation frequency (rad/s), i is square root of -1, $s(\omega)$ and $jk(\omega)$ are the small-signal photon density and current density, respectively.

A similar expression can be obtained for the CRVCL modulation response when only the bottom cavity is under direct modulation, as shown in (3) at the bottom of this page.

If the coupled cavities are exactly identical (e.g., same laser gain, differential gain, longitudinal mode distribution, etc.), the modulation responses (1) and (3) can be simplified, producing the same modulation response as that of a conventional VCSEL [2]. Otherwise, we show in this study that the asymmetries between the coupled cavities play a role in determining the CRVCL modulation response. These asymmetries can be exploited to engineer the CRVCL modulation response, and ultimately, to achieve a higher modulation bandwidth than that of a conventional VCSEL. In practice, the asymmetries between the coupled cavities can be varied by the CRVCL epitaxial structure and/or the dc operation points. Here, we demonstrate that cavity detuning, which governs the longitudinal mode distribution within a CRVCL, can be used to produce the cavity asymmetry and to engineer the modulation response.

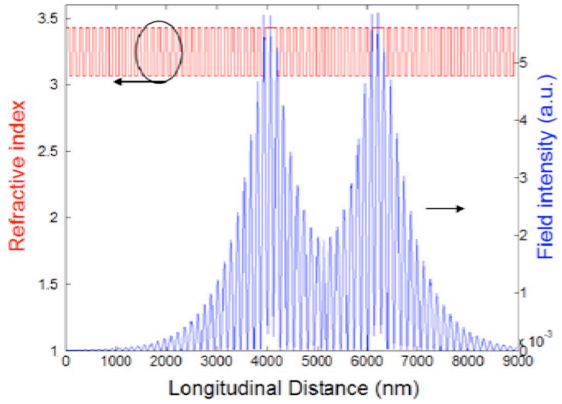

Fig. 2. Calculated refractive index and normalized optical field intensity for the short-wavelength longitudinal mode along the growth direction of a CRVCL, when the top and bottom cavities have the same optical path length.

The cavity detuning is a unique property of the coupled-cavity structure, which allows a longitudinal optical mode to preferentially distribute toward one cavity or the other. Fig. 2 illustrates the calculated optical field distribution in a CRVCL for the shorter wavelength longitudinal mode. The percentage of the optical field overlapping with the top and bottom cavity is denoted as ξ_1 and ξ_2, respectively. If the two CRVCL cavities have the same optical path length, the longitudinal mode distribute equally between the two cavities, and thus ξ_1 and ξ_2 are equal to 50% (see Fig. 2). Note that the total photon density in a CRVCL is constant, i.e., $\xi_1 + \xi_2 = 1$. The two cavities can also be detuned from each other, such that one cavity can have a longer optical path length than the other. The optical field of the shorter wavelength longitudinal mode shifts toward the laser facet (substrate), when the top cavity has a shorter (longer) optical path length than the bottom cavity [7].

Fig. 3(a) shows the CRVCL modulation response as a function of the percentage of the optical longitudinal mode overlapping with the top cavity (ξ_1), when only the top cavity is under direct modulation. The modulation response is calculated using (1), and the device parameters used in the calculation taken from [8] are summarized in Table I. The calculations shown in Fig. 3(a) only vary ξ_1 and assume the other cavity parameters are the same for both cavities. It can be observed from Fig. 3(a) that the modulation response has an increasing relaxation oscillation (RO) peak and greater modulation bandwidth as more optical field is confined in the top cavity. On the other hand, Fig. 3(b) shows the CRVCL modulation response as a function

$$\left|\frac{s(\omega)}{j_1(\omega)}\right| = \left|\frac{\Gamma_1 v_1 g'_1 S_0/qd_1}{\omega^2 + i\omega(1/\tau_1 + v_1 g'_1 \xi_1 S_0) - v_1^2\Gamma_1\xi_1 g_1 g'_1 S_0 - v_2^2\Gamma_2\xi_2 g_2 g'_2 S_0\gamma}\right| \tag{1}$$

$$\gamma = \frac{i\omega - (1/\tau_1 + v_1 g'_1 \xi_1 S_0)}{i\omega - (1/\tau_2 + v_2 g'_2 \xi_2 S_0)}. \tag{2}$$

$$\left|\frac{s(\omega)}{j_2(\omega)}\right| = \left|\frac{\Gamma_2 v_2 g'_2 S_0/qd_2}{\omega^2 + i\omega(1/\tau_2 + v_2 g'_2 \xi_2 S_0) - v_2^2\Gamma_2\xi_2 g_2 g'_2 S_0 - v_1^2\Gamma_1\xi_1 g_1 g'_1 S_0/\gamma}\right|. \tag{3}$$

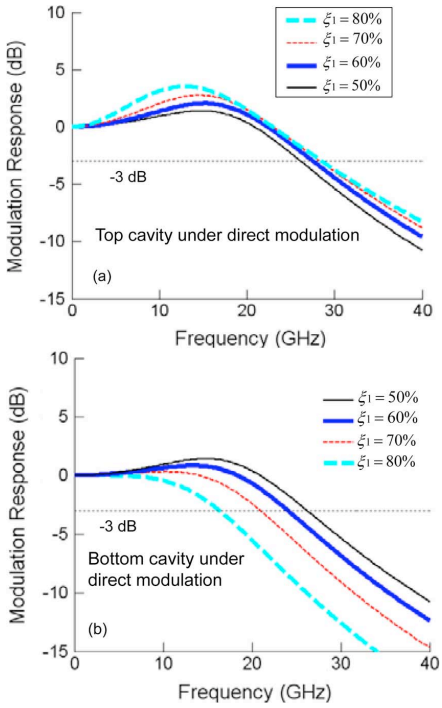

Fig. 3. CRVCL modulation response as a function of the fraction of the longitudinal optical field in the top cavity, when the (a) top and (b) bottom cavity is under direct modulation. A fixed photon density is assumed.

TABLE I
DEVICE PARAMETER VALUES USED DURING CALCULATION, UNLESS NOTED OTHERWISE

Γ	Optical confinement factor	0.0382
τ_1, τ_2	Carrier lifetime (ns)	2.6
τ_p	Photon lifetime (ps)	2.5
g_1', g_2'	Differential gain (cm^{-2})	10^{-16}
g_1, g_2	Gain coefficient (cm^{-1})	800
S_0	Photon density (cm^{-3})	4×10^{16}
v	Group velocity (cm/s)	$3/3.5\times10^{10}$

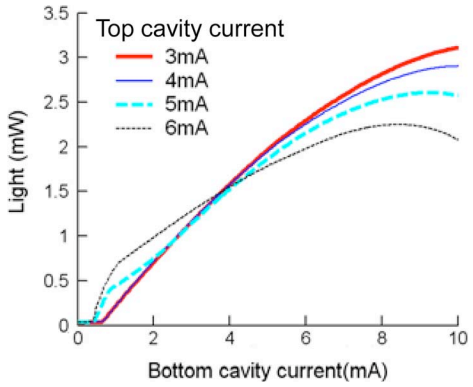

Fig. 4. LI characteristics of the bottom cavity with different top cavity currents.

of ξ_1, when only the bottom cavity is under direct modulation. The modulation response is calculated using (3). Similarly, the modulation response can be engineered by varying the detuning between both cavities. However, it is interesting to observe that the modulation response exhibits the opposite trend as compared to Fig. 3(a). The thin solid curves in Fig. 3(a) and (b) correspond to the same modulation response, which is also equivalent to the modulation response of a conventional VCSEL with the same photon density. When more optical field is confined in the top cavity, the modulation response becomes more damped (decreasing RO peak) and the modulation bandwidth decreases. Therefore, for a given ξ_1, we can obtain two different modulation responses, depending on which cavity we have chosen to apply direct modulation. For an appropriate ξ_1, the CRVCL would achieve a larger bandwidth than that of a conventional VCSEL with the same photon density. This is consistent with the observation obtained in prior work [2]. The dependence of the modulation responses on ξ_1 in Fig. 3 can be explained by analyzing the poles and zeros of (1) and (3) [9].

The maximum bandwidth achieved from our CRVCL devices using the direct modulation in a single cavity is 23 GHz. This particular CRVCL is fabricated from a wafer composed of a bottom p-type DBR with 35 periods, an n-type middle mirror, and an upper p-type DBR with 18 periods. The middle mirror contains 6.5-period DBR and a one-wavelength-thick GaAs contact layer. The top and bottom optical cavities contain 7 $GaAs/Al_{0.2}Ga_{0.8}$ As quantum wells emitting nominally at 850 nm. An 11×11 μm^2 implant and 5×5 μm^2 oxide aperture are formed in the upper and bottom mesa, respectively. The CRVCL shows unusual light–current (LI) characteristics in that the light power decreases (for the bottom cavity current larger than 4.5 mA) with increasing dc current in the top cavity (see Fig. 4). These unusual LI characteristics can be attributed to the variation of the longitudinal mode distribution with increasing injection current in the top cavity. The CRVCL emits predominantly on the shorter-wavelength longitudinal mode, but has multiple transverse modes [10].

Fig. 5(a) illustrates the measured small-signal responses with different bottom cavity current. The RO frequency increases with the increasing bottom cavity current, and thus with the increasing photon density. The contour map in Fig. 5(b) shows the dependence of the -3 dB bandwidth on the top and bottom cavity current. This map consists of 40 measurement points. For each point, the modulation response, and thus the -3 dB bandwidth, is measured at a given combination of the top and bottom cavity current. The change of the bottom cavity current leads to a more significant change in the modulation bandwidth than does the top cavity current for this particular CRVCL.

B. Direct Modulation Using Two Cavities

As mentioned earlier, the CRVCL can also be modulated by applying direct modulation to both cavities simultaneously. It was found in [6] and[7] that the total modulation response is a superposition of the direct modulation response from each individual cavity. Assume the small signal current $j_1(\omega)$ and $j_2(\omega)$ are related by the following expression

$$j_1(\omega) = Ae^{i\theta} j2(\omega) \tag{4}$$

where A and θ are the amplitude and phase difference between the small-signal currents injected in the cavities, the total mod-

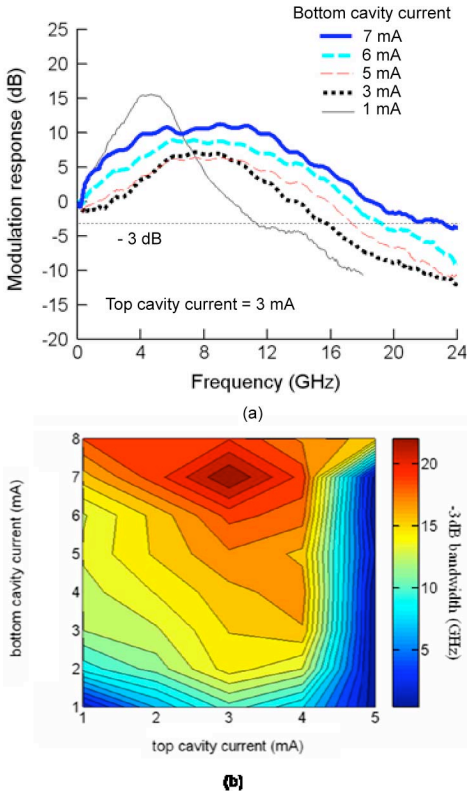

Fig. 5. (a) Measured small-signal responses with different bottom cavity current. (b) Dependence of the modulation bandwidth on the top and bottom cavity current.

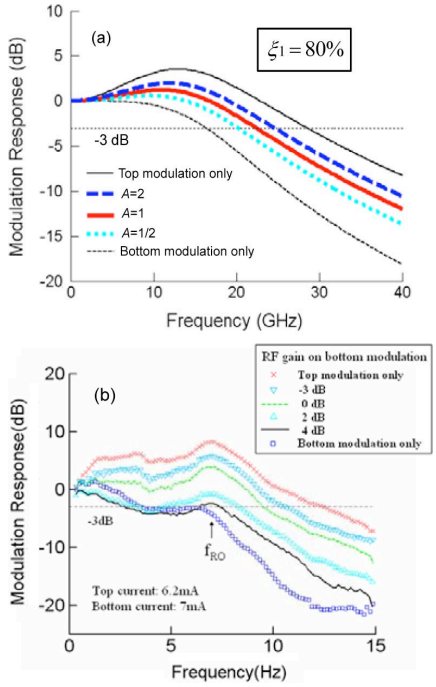

Fig. 6. (a) Calculated modulation responses with different A for a fixed detuning. The modulation responses from the individual cavity are also plotted for reference. A fixed photon density is assumed. (b) Measured modulation responses as the relative modulation amplitude in both cavities varied by an RF attenuator.

ulation response found from (1) and (3) can be written as in (5) at the bottom of this page.

As shown in Fig. 3, the direct modulation response from the top and bottom cavity will split as the cavity detuning increases, and the modulation response can be engineered by varying the cavity detuning. However, when both cavities are under simultaneous direct modulation, we find that the total modulation response can be engineered even for a fixed cavity detuning. Fig. 6(a) shows the calculated total modulation response at different amplitude ratios between the two modulation signals A. For a fixed cavity detuning ($\xi_1 = 80\%$ in this case), the total response can be tailored by varying A. Thus, an optimal response can be achieved by making a tradeoff between the RO peak and the -3 dB modulation bandwidth. The range of the total modulation response is set by the two modulation responses from the individual cavities.

Fig. 6(b) illustrates the measured modulation characteristics from a CRVCL fabricated from a wafer that consists of a monolithic bottom p-type DBR with 35 periods, a middle n-type DBR with 12.5 periods, and an upper p-type DBR with 22 periods [6]. The experimental results in Fig. 6(b) are consistent with the calculated results from the small-signal model in Fig. 6(a). The differential series resistance of this CRVCL is 590 and 205 Ω in the top and bottom cavity, respectively.

C. Push–Pull Modulation

Push--pull modulation requires the CRVCL cavities to be directly modulated by two out-of-phase electrical signals [7]. Because the cavities are typically not identical, the amplitude ratio between the two direct modulation signals are adjusted such that there is no net change in the carrier and photon densities inside the laser, and thus the RO frequency will be suppressed. The laser output modulation occurs due to the variation the longitudinal mode profile in the cavities induced by the carrier mediated refractive index in each cavity. Fig. 2 shows the profile of the longitudinal mode distribution. Under appropriate conditions, the longitudinal optical mode is either "pushed" toward the laser output facet, producing higher output power, or is "pulled" toward the substrate side, producing lower output power. Thus, with unchanged photon density inside the laser, different light intensity is coupled out from the CRVCL, and the light output modulation arises from modulation of the longitudinal optical mode distribution.

For small-signal analysis, the push--pull modulation can be treated as a special case of (5), where $j_1(\omega) = -j_2(\omega)$. Under this condition, the total modulation response $|(s(\omega))/(j_2(\omega))|$

$$\left|\frac{s(\omega)}{j_2(\omega)}\right| = \left|\frac{Ae^{i\theta}\Gamma_1 v_1 g_1' S_0/qd_1 + \Gamma_2 v_2 g_2' S_0/qd_2\gamma}{\omega^2 + i\omega(1/\tau_1 + v_1 g_1' \xi_1 S_0) - v_1^2\Gamma_1\xi_1 g_1 g_1' S_0 - v_2^2\Gamma_2\xi_2 g_2 g_2' S_0\gamma}\right|. \quad (5)$$

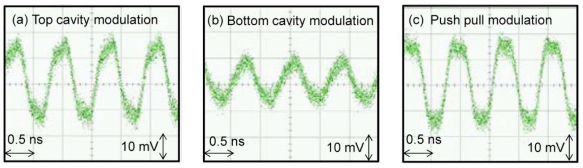

Fig. 7. Optical output signal at 2.5 Gb/s, when the (a) top and (b) bottom cavity are under direct modulation, (c) when both cavities are under direct modulation simultaneously at the push--pull condition.

is equal to 0. This means the exact push--pull condition of $A = 1$ and $\theta = \pi$ corresponds to no light modulation. However, the modulation of the longitudinal mode distribution is neglected for this analysis, because it is not naturally included in the CRVCL rate equations. A rigorous rate-equation model that can account for dynamical variation of the longitudinal mode distribution is under investigation.

In order to demonstrate the push--pull modulation, large-signal characteristics of the CRVCL are measured at 2.5 Gb/s [7]. Fig. 7(a) and (b) illustrates the measured optical output signal, when only the top and bottom cavity is subject to direct modulation, respectively. Fig. 7(c) shows the optical signal when both cavities are under direct modulation simultaneously but 180° out-of-phase. In the absence of push--pull operation, we would expect to observe a flat signal in Fig. 7(c) indicating no modulation. However, modulation is observed with an extinction ratio of 1.27 dB. Examination of the relative intensity noise (RIN) spectra when the CRVCL is operating at the push, pull, and quiescence state shows the RO frequencies are identical, indicating no change in the total photon density inside the CRVCL, and a calibration is performed to ensure that modulation occurs between the predetermined push and pull states [7]. However, bandwidth enhancement of the push--pull modulation is not apparent in a small-signal measurement, due to the large electrical parasitics of our current CRVCLs [7].

D. Electroaborption Modulation

Instead of applying direct modulation, the CRVCL laser output can also be modulated by varying the electroabsorption in an optical cavity, owing to the quantum-confined Stark effect from quantum wells. However, the CRVCL shows considerably different modulation characteristics under electroabsorption modulation, producing not only a potentially larger modulation bandwidth but also a larger RO peak than those from direct modulation [5]. In Fig. 8, the direct or electroabsorption modulation is applied to the bottom or top cavity, respectively. The fitted curves are calculated using (3) and the model proposed in [5] for the direct and electroabsorption modulation, respectively. Note that the model in [5] does not fully account for the coupled-cavity asymmetries, causing the calculated response to deviate below 3 GHz. The large RO peak from the electroabsorption modulation can severely limit the large-signal modulation speed of the CRVCL [5]. In order to flatten the modulation response, the electroabsorption modulation can be applied simultaneously with the direct modulation through the coupled cavities [9], [11].

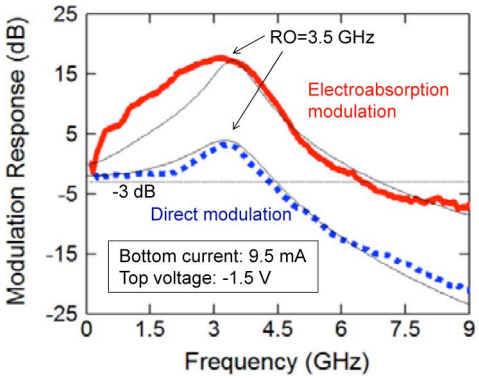

Fig. 8. Comparison of the measured direct and electroabsorption modulation responses using a single-CRVCL cavity. Thin solid lines are the fitted responses.

III. Analog and Digital Functionalities

A. Multilevel Amplitude Modulation

Multilevel amplitude modulation is widely used in digital communications to achieve higher spectra efficiency than the conventional binary OOK modulation [12]. Multilevel amplitude modulation, specifically four-level pulse amplitude modulation (PAM-4) of a VCSEL has been explored in prior work, as an alternative approach to achieve higher speed digital modulation [13]. PAM-4 signaling also has the ability to mitigate frequency-dependent attenuation and fiber dispersion and thus lower the link budget [14]. in addition, PAM-4 signaling offers an advantage in VCSEL reliability, because it requires lower modulation bandwidth and thus smaller current density for a given data rate as compared to OOK modulation [13]. However, PAM-4 signaling also increases the complexity of the design and implementation of VCSEL driver circuits, preventing the widespread of system-level evaluation of VCSEL-based PAM-4 signaling.

The CRVCL has advantages for PAM-4 signaling. As shown in Fig. 6, the total modulation response is a superposition of the individual responses from the top and bottom cavities. This unique property enables the CRVCL to produce a PAM-4 optical signal by combining two binary amplitude modulation electrical signals in the coupled cavities [6]. Moreover, CRVCL doesn't require complex driver circuits to produce a PAM-4 signal. Instead each CRVCL cavity can be driven by binary signaling circuits that are simpler to implement.

Fig. 9 illustrates the experimental results of PAM-4 signaling of a CRVCL [6]. Fig. 9(a) and (b) illustrates the 2.5 and 1.25 GHz square-wave electrical signal applied to the top and bottom cavity, respectively. Fig. 9(c) shows the optical output signal is consisted of four amplitude levels, as a result of adding the individual modulation responses from the top and bottom cavity. The highest (or lowest) amplitude level denoted as 11 (or 00) is achieved when both input signals are switched high (or low). The intermediate level 10 and 01 corresponds to the individual modulation response from the bottom and top cavity, respectively. Fig. 9(d) shows the optical waveform after applying 6 dB RF attenuation to the modulation signal to the top cavity. The relative amplitude for the intermediate levels 10 and 01 vary between Fig. 9(c) and (d), as the amplitude of the modulation response from the top cavity decreases with the RF attenuation.

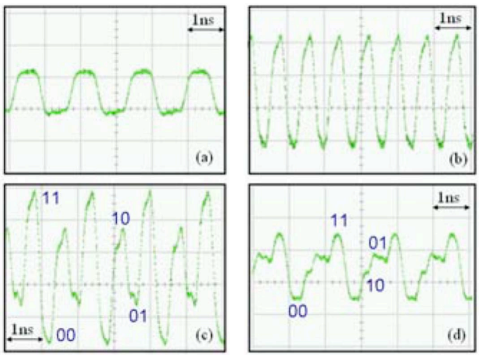

Fig. 9. Optical output signal when only the (a) bottom and (b) top cavity is under direct modulation. Optical output signal when (c) 0-dB and (d) 6-dB attenuation is applied to the top cavity, given that both cavities are under direct modulation simultaneously.

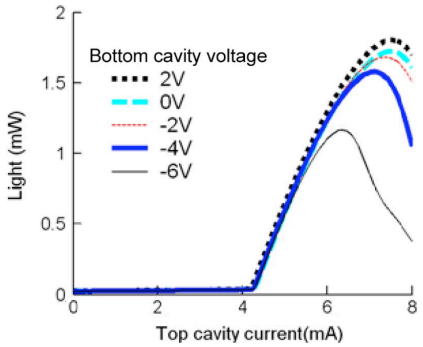

Fig. 10. Light output versus top cavity current with different dc voltages on the bottom cavity.

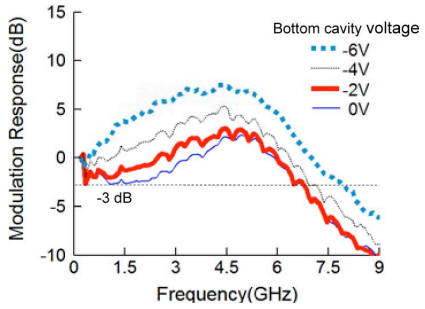

Fig. 11. Small-signal modulation characteristics of the CRVCL with 7 mA current applied to the top cavity and different dc voltages applied to the bottom cavity.

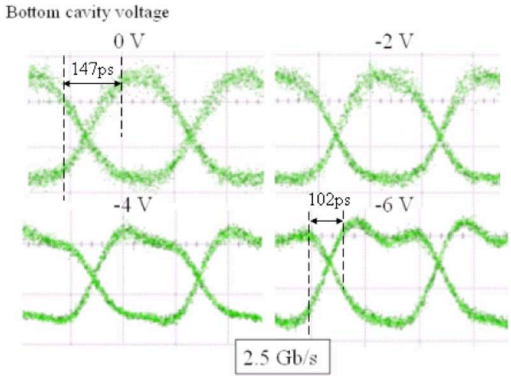

Fig. 12. Large-signal modulation characteristics at 2.5 Gb/s with different dc voltages on the bottom cavity. The 10%–90% rise times are shown for 0 and −6 V bottom cavity voltage.

B. Preemphasis for Direct Modulation

For high-speed digital communication, preemphasis or equalization is often applied to transmitter or receiver, in order to compensate for signal distortion arising from the transmission medium. It was found in prior work that VCSEL bandwidth and transmission distance can be increased by using integrated circuits with the preemphasis capability [15]. It is demonstrated here that the coupled-cavity structure can be directly utilized to pre-emphasize the VCSEL modulation. In order to introduce preemphasis, the direct modulation is applied to one cavity, and the other cavity is then biased to less than transparency so that it has optical loss from electroabsorption. The dc component of the modulation signal is suppressed by increasing the electroabsorption loss in the cavity, and thus the modulation response will be enhanced relative to its dc value. The strength of the electroabsorption can be varied by the voltage applied to the loss cavity.

Fig. 10 illustrates the light versus top cavity current for different dc voltages on the bottom cavity. The light output decreases and threshold current slightly increases, as a larger reverse voltage is applied to the bottom cavity creating increasing electroabsorption. Fig. 11 illustrates the small-signal CRVCL modulation responses for 7 mA fixed current injected into the top cavity and different bottom cavity voltages. As larger reverse voltage is applied to the bottom cavity, the modulation response has increased modulation bandwidth and more pronounced RO peak, because the low frequency component of the modulation signal is suppressed from the electroabsorption in the bottom cavity. For example, the application of −6 V suppresses the modulation response at 200 MHz by 12 dB. By varying the bottom cavity voltage, the strength of the electroabsorption can be adjusted and thus the overall modulation response from the CRVCL can be varied.

Fig. 12 illustrates the large-signal characteristics at a data rate of 2.5 Gb/s with different bottom cavity voltages. With no preemphasis (no voltage applied to the bottom cavity) the rise time in Fig. 11 is 147 ps. When −6 V is applied to the bottom cavity the rise time decreases to 102 ps. The rising edges of the large signals are emphasized as a result the increasing electroabsorption, which corresponds to the increasing RO peak in the small-signal modulation responses. The result of the preemphasis is a more open eye diagram, as shown in Fig. 11. Optimization of the coupled-cavity structure could further reduce laser loss and achieve higher modulation rate.

C. Microwave Signal Mixing

In addition to digital modulation applications, the CRVCL has also exhibited new analog functionality to perform microwave signal mixing within its coupled optical cavities [16]. When two microwave signals of different frequencies are launched into a CRVCL through the top and bottom cavity, signal mixing takes place inside the laser cavity, which can be observed from the RF spectrum of the laser output, using a broadband RF spectrum analyzer. Signal mixing generates RF signals at new frequencies, making the CRVCL useful for frequency conversion in a radio-over-fiber transmission system.

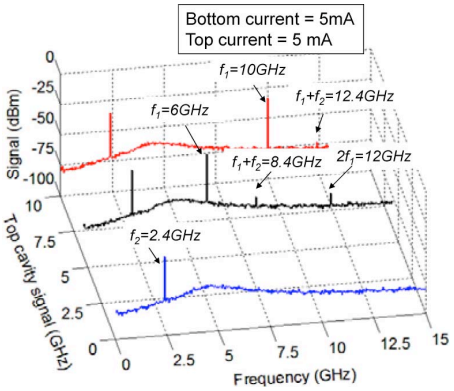

Fig. 13. RF spectra of the CRVCL light output as a function of RF frequency injected into the top cavity, when the RF frequency in the bottom cavity is 2.4 GHz. Both the top and bottom cavity current are fixed at 5 mA.

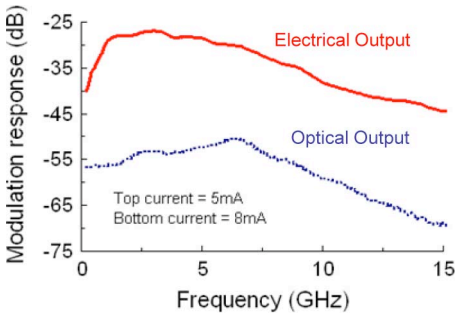

Fig. 14. Small-signal modulation responses (not normalized) for the electrical and optical output ports.

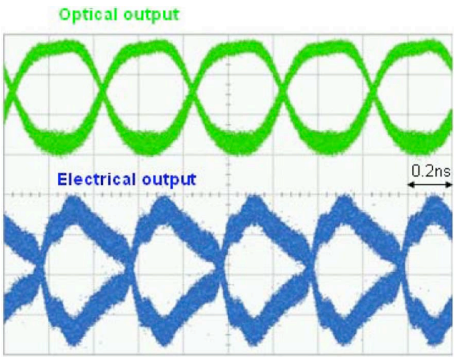

Fig. 15. Large-signal modulation responses for the electrical and optical output ports.

The same CRVCL, as shown in Fig. 6(a), is used for the signal mixing experiment. Fig. 13 illustrates the RF spectra of the CRVCL output while varying the frequency of the microwave signal applied to the top cavity f_1, when the signal injected into the bottom cavity is fixed at the frequency $f_2 = 2.4$ GHz with a RF power of -25 dBm. Only one signal peak at 2.4 GHz is present in the RF spectrum, if no signal is applied to the top cavity. The mixed signal at $f_1 + f_2 = 8.4$ GHz (or 12.4 GHz) is observed, when the signal $f_1 = 6$ GHz (or 10 GHz) with -3 dBm (or 20 dBm) RF power is injected into the top cavity. For $f_1 = 10$ GHz, a large RF power is injected to compensate for the decayed modulation response at frequencies higher than the RO frequency, so that the mixed signal at $f_1 + f_2 = 12.5$ GHz can be observed. It is apparent from Fig. 13 that the CRVCL performs the frequency conversion from f_2 to $f_1 + f_2$, and the converted frequency is a function of the microwave frequency injected in the top cavity. This frequency mixing functionality of the CRVCL would enable the same transmission system as in [17] in a compact manner with no need of an electrical mixer. Note that both signal addition (see Fig. 9) or signal mixing (see Fig. 13) has been achieved in the same CRVCL device, using different bias and modulation signal power. Thus, optimization of the dc biasing condition and the modulation signal power is often required for different CRVCL functionalities.

D. Synchronous Electrical and Optical Signaling

As a three-terminal optoelectronic device, the CRVCL has two electrical ports and one optical port. For the CRVCL applications shown in the previous sections, when the input signals are applied to the two electrical ports, the optical signal can be produced and even tailored at the optical port. A different configuration is explored here, where only one electrical port is used as the input port, and the other electrical port and the optical port are both used as the output ports in order to produce simultaneous electrical and optical signaling. Either the top or bottom cavity can be used as the input electrical port.

The photon population in a CRVCL is coupled with the carrier densities in both optical cavities through the stimulated recombination. The variation of the photon density will thus result in the variation of the carrier density in both cavities, no matter whether a single cavity or both cavities are under direct modulation. This unique ability enables the CRCVL to produce synchronous electrical and optical output signal, and thus it may facilitate some board- or chip-level device applications that interface the optical and electrical information for signal processing and data communications. For example, while the optical signal is transmitted to a remote board or chip via optical fiber, waveguide, or free space, the electrical signal can be routed locally to perform logic functions or modulate other optoelectronic devices.

For large-signal measurement, the modulation signal is applied to the input electrical port from a pattern generator, and the electrical and optical output can be measured simultaneously on two different channels of an oscilloscope. For small-signal measurement, the modulation responses from the electrical and optical ports need to be measured separately. To measure the scattering parameter for the optical port, a multimode fiber and a high-speed photodetector are used to collect output light from the CRVCL, and then the photodetector output is connected to the network analyzer. To measure the scattering parameter for the electrical port, the electrical output from a ground-signal pair of the GSSG coplanar contact is connected directly to the network analyzer via a bias tee.

The same CRVCL, as shown in Fig. 6(b), is used in this experiment. Fig. 14 illustrates the small-signal responses for both the electrical and output port. The dc current for the top and bottom cavity is 5 and 8 mA, respectively. The modulation signal is applied to the top cavity to achieve a larger optical modulation bandwidth (11 GHz). The electrical port has a slightly larger modulation bandwidth (14 GHz). The high insertion loss from the electrical port is partly due to the large differential series resistance of the CRVCL cavities. Fig. 15 illustrates the large-signal responses for the electrical and optical

output ports at 2.5 Gb/s. The optical signal shows a high-quality eye diagram. However, the electrical signal produces an eye of marginal quality, due to the rise of the modulation response at low frequencies.

IV. Conclusion

In this paper, we have presented an overview of the modulation approaches for the CRVCL, with an emphasis on direct modulation using either or both cavities of the CRVCL. For direct modulation using a single cavity, the cavity detuning has a significant impact on the modulation responses; a maximum bandwidth of 23 GHz is demonstrated. For direct modulation using both cavities, the amplitude and/or phase difference between the modulation currents are used to engineer the CRVCL modulation response. Push--pull modulation is demonstrated, when the amplitude difference between the two exactly out-of-phase modulation currents is adjusted such that there is no net change in the carrier and photon densities inside the CRVCL; the CRVCL produces light modulation by spatially varying the longitudinal optical mode distribution. This modulation approach is inherently decoupled from changes of the photon density, so increasing photon density is not necessary for increasing the modulation bandwidth. Finally, with the unique modulation properties, the CRVCL has demonstrated new analog and digital functionalities. The CRVCL can be used to produce multilevel amplitude modulation, preemphasis for direct modulation, microwave signal mixing, or synchronous electrical and optical signaling. None of these applications are possible using a conventional VCSEL. With optimization of the CRVCL structure and reduction of electrical parasitics, the CRVCL may be a promising laser source for many emerging applications, where additional functionality and low power operation are desired.

Acknowledgment

The authors would like to thank A. Allerman from Sandia National Laboratories for epitaxial materials, and M. Hibbs-Brenner, K. Johnson, and P. Crump for technical discussions.

References

[1] K. D. Choquette and K. M. Geib, , C. Wilmsen, H. Temkin, and L. Coldren, Eds., "Fabrication and performance of vertical-cavity surface-emitting lasers," in *Vertical-Cavity Surface-Emitting Lasers*. New York: Cambridge University Press, 1999, pp. 193–232.

[2] D. M. Grasso, D. K. Serkland, G. M. Peake, K. M. Geib, and K. D. Choquette, "Direct modulation characteristics of composite resonator vertical-cavity lasers," *IEEE J. Quantum Electron.*, vol. 42, no. 12, pp. 1248–1254, Dec. 2006.

[3] V. A. Shchukin, N. N. Ledentsov, J. A. Lott, H. Quast, F. Hopfer, L. Ya. Karachinsky, M. Kuntz, P. Moser, A. Mutig, A. Strittmatter, V. P. Kalosha, and D. Bimberg, "Ultra high-speed electro-optically modulated VCSELs: Modeling and experimental results," in *Proc.SPIE*, 2008, vol. 6889, pp. 68890H-1–68890H-15.

[4] J. van Eisden, M. Yakimov, V. Tokranov, M. Varanasi, E. M. Mohammed, I. Young, and S. Ortyabrsky, "Optical decoupled loss modulation in a duo-cavity VCSEL," *IEEE Photon. Technol. Lett.*, vol. 20, no. 1, pp. 42–44, Jan. 2008.

[5] C. Chen, P. O. Leisher, D. M. Grasso, C. Long, and K. D. Choquette, "High-speed electroabsorption modulation of composite-resonator vertical-cavity lasers," *IET Optoelectron.*, vol. 3, no. 2, pp. 93–99, 2009.

[6] C. Chen and K. D. Choquette, "Multilevel amplitude modulation using a composite-resonator vertical-cavity laser," *IEEE Photon. Technol. Lett.*, vol. 21, no. 15, pp. 1030–1032, Aug. 2009.

[7] C. Chen, K. L. Johnson, M. Hibbs-Brenner, and K. D. Choquette, "Push-pull modulation of a composite-resonator vertical-cavity laser," *IEEE J. Quantum Electron.*, to be published.

[8] L. A. Coldren and S. W. Corzine, *Diode Lasers and Photonic Integrated Circuits*. New York: Wiley, 1995.

[9] C. Chen, "Coupled cavity surface emitting lasers: modulation concepts, performance and applications," Ph.D. dissertation, Univ. Illinois Urbana-Champaign, Urbana, 2009.

[10] A. C. Lehman and K. D. Choquette, "Threshold gain temperature dependence of composite resonator vertical cavity lasers," *IEEE J. Sel. Topics Quantum Electron.*, vol. 11, no. 5, pp. 962–967, Sept./Oct. 2005.

[11] E. A. Avrutin, V. B. Gorfinkel, S. Luryi, and K. A. Shore, "Control of surface-emitting laser diodes by modulating the distributed Bragg mirror reflectivity: Small-signal analysis," *Appl. Phys. Lett.*, vol. 63, no. 18, pp. 2460–2462, 1993.

[12] J. G. Proakis and M. Saleshi, *Communication Systems Engineering*. Englewood Cliffs, NJ: Prentice Hall, 2002.

[13] J. E. Cunningham, D. Beckman, X. Zheng, D. Huang, T. Sze, and A. V. Krishnamoorthy, "PAM-4 signaling over VCSELs with 0.13 μm CMOS chip technology," *Opt. Exp.*, vol. 14, no. 25, pp. 12028–12038, 2006.

[14] S. Walkin and J. Conradi, "Multilevel signaling for increasing the reach of 10 Gbps systems," *J. Lightw. Technol.*, vol. 17, no. 11, pp. 2235–2248, Nov. 1999.

[15] D. Kuchta, P. Pepeljugoski, and Y. Kwark, "VCSEL modulation at 20 Gb/s over 200 m of multimode fiber using a 3.3 v SiGe laser driver IC," in *Tech. Dig. LEOS Summer Topical Meetings*, Jul. 2001, pp. 49–50.

[16] C. Chen and K. D. Choquette, "Microwave frequency conversion using a coupled-cavity surface-emitting laser," *IEEE Photon. Technol. Lett.*, vol. 19, no. 21, pp. 1393–1395, 2009.

[17] N. K. Dutta, M. Tayahi, and K. D. Choquette, "Transmission experiments using oxide confined vertical cavity surface emitting lasers," *Electron. Lett.*, vol. 33, no. 13, pp. 1147–1148, 1997.

Chen Chen (S'07) received the B.S., M.S., and Ph.D. degrees in electrical and computer engineering from the University of Illinois at Urbana-Champaign, in 2004, 2006, and 2009, respectively.

He was engaged in research on high-speed modulation of vertical cavity surface emitting lasers (VCSELs) and coupled-cavity VCSELs. He is currently a Postdoctoral Researcher with the Photonics Systems Group, Department of Electrical and Computer Engineering, McGill University, Montreal, QC, Canada, where he is engaged in research on modulation formats, signal processing, and optoelectronic devices for optical communications. He is the author or coauthor of more than 30 papers published in peer-reviewed journals and conferences.

Kent D. Choquette (M'97–F'03) received the Ph.D. degree in materials science from the University of Wisconsin-Madison, Madison.

He is currently a Professor in the Electrical and Computer Engineering Department, University of Illinois, Urbana. He is the author or coauthor of more than 200 technical publications and three book chapters, and has presented numerous invited talks and tutorials.

Dr. Choquette is a Fellow of the Optical Society of America and the International Society for Optical Engineers. He has been served as an Associate Editor of the IEEE Journal of Quantum Electronics, IEEE Photonics Technology Letters, and IEEE/OSA Journal of Lightwave Technology, and a Guest Editor of the IEEE Journal of Selected Topics in Quantum Electronics. He was the recipient of the 2008 IEEE/Laser and Electro-Optics Society Engineering Achievement Award.